Am J Cancer Res 2012;2(2):168-177
www.ajcr.us /ISSN:2156-6976/ajcr0000101

Original Article

Tumor growth is suppressed in mice expressing a truncated XRCC1 protein

Christina Pettan-Brewer[1], John Morton[1], Sarah Cullen[1], Linda Enns[1], Keffy RM Kehrli[2], Julia Sidorova[2], Jorming Goh[1], Rebecca Coil[1], Warren C Ladiges[1]

[1]Departments of Comparative Medicine, School of Medicine, University of Washington, Seattle, WA 98195; [2]Departments of Comparative Pathology, School of Medicine, University of Washington, Seattle, WA 98195

Received January 3, 2012; accepted January 30, 2012; Epub February 15, 2012; Published February 28, 2012

Abstract: Tumor progression depends on the support of cells in the microenvironment, and is driven in part by the generation of reactive oxygen species (ROS). ROS can damage DNA, and the repair of damaged DNA is a well-known process involved in tumor initiation and promotion, but the role of DNA repair in tumor progression is not fully understood. In this regard the X-ray cross complementing 1 (XRCC1) protein is known to orchestrate the assembly of repair complexes at sites of DNA single strand breaks either directly or indirectly through repair of damaged bases, largely as the result of ROS-induced damage. XRCC1 polymorphisms have been shown to be associated with increased cancer. It was therefore of interest to investigate the effect of XRCC1 gene mutations on cancer progression. In an attempt to make XRCC1 point mutant mice, we generated a truncated protein (XRCC1tp) by the insertion of a neomycin cassette in intron12 of the XRCC1 gene. This unique finding allowed us to investigate cellular and tumor progression phenotypes in mice associated with expression and function of an altered XRCC1 protein on one allele. XRCC1tp cells showed increased toxicity to MMS, enhanced MMS-induced depletion of NADH suggesting increased PARP activity, and normal functional repair of MMS-induced DNA damage. Six months following treatment with the alkylating carcinogen azoxymethane (AOM) at 10 mg/kg once a week for 6 weeks, XRCC1tp mice had a decrease in average colon tumor volume of 14±3 mm^3 compared to 34±4 mm^3 in WT littermates ($p \leq 0.03$, N= 20/genotype). XRCC1tp mice had a 72 per cent decrease in B16 melanoma tumor burden compared to wt littermates. Average tumor volume in transgenic PyMT metastatic breast cancer mice expressing XRCC1tp was 359 cubic mm in PyMT mice expressing XRCC1tp compared to 730 cubic mm in PyMT mice expressing XRCC1wt ($p \leq 0.001$, N= 20/genotype). These data suggest that the presence of an XRCC1 truncated protein alters XRCC1 function independent of DNA repair, and is associated with anti-tumor activity.

Keywords: Tumor suppression, XRCC1, melanoma, colon cancer, breast cancer, PARP, apoptosis

Introduction

Tumor progression is under the control of a number of factors including those directed by tumor cells and those directed by the tumor microenvironment in response to tumor cell signaling. The events are designed to enhance the invasive characteristics of the tumor cells and assure that they continue to proliferate. The repair of damaged DNA is a well-known process involved in tumor initiation and promotion, but the role of DNA repair in tumor progression is not fully understood. Tumor progression depends on the support of cells in the microenvironment and cell cycle response to tumor cytokines, but reactive oxygen species (ROS) could cause DNA damage and a DNA damage response that alters this response. The X-ray cross complementing 1 (XRCC1) protein is a DNA repair protein that is responsive to ROS-indcued DNA damage and functions to orchestrate the assembly of repair complexes at sites of DNA single strand breaks either directly, or indirectly through repair of damaged bases [1]. XRCC1 has no known catalytic activity, but appears to play an essential role as a scaffolding protein which can physically interact with other proteins, such as PARP, POL beta and Ligase III [2-5], and facilitate enzymatic activities. Epidemiology studies have reported an association of XRCC1 polymorphisms with cancer [6] so it is of interest to investigate function in the context of

tumor progression in a model system.

During the course of generating mouse lines expressing XRCC1 point mutations, we observed a truncated protein in one mouse line with a neomycin cassette inserted into intron12. Both human and mouse XRCC1 genes contain 17 exons and encode proteins of 633 and 631 amino acids, respectively which are 84% identical within the coding regions, and 86% similar at the amino acid sequence level [7]. Intron and exon lengths are highly conserved, so that the mouse is an excellent model to study the comparative aspects of XRCC1 gene function. We describe in this paper an anti-tumor phenotype that provides a novel animal model to study tumor progression and XRCC1 function.

Materials and methods

Mouse lines and tumor models

The neomycin cassette vector was generated using standard molecular biology cloning techniques by contractual arrangement with Vector Biolabs (Philadelphia, PA). Genetically targeted mice were generated as previously described [8]. Briefly, we used a C57BL/6 ES cell line to generate targeted clones for making chimeric mice, which were then tested for germline transmission and subsequent genotyping and phenotyping. Heterozygous males were backcrossed to C57BL/6 females.

For azoxymethane challenge, four-month-old XRCC1tp and wild type male mice (N=18 for each genotype) were injected with 10 mg/kg azoxymethane (AOM, Sigma) intraperitoneally, once a week for six weeks. An equal number of wild type littermates were injected with sterile diluent only. All mice were monitored and weighed weekly and terminated six months following the last AOM treatment. Colons were removed and flushed with phosphate-buffered saline and the tumors were counted and measured with a digital caliper. The distended colons were fixed overnight in 10% neutral buffered formalin or harvested and snap-frozen. Tumor volumes were calculated as length × width^2 × π/6. The position of each tumor along the length of the colon was recorded. Sections were stained with hematoxylin and eosin according to standard protocol.

For melanoma implantation, four-month-old cohorts consisting of 20 XRCC1 mutant mice and 20 wild type littermates were divided into half and one half continued on standard rodent chow and one half fed a Surwit diet (No. F3282; Bio-Serv, Frenchtown, NJ) for two months. The Surwit diet is high in fat and sugar containing 35% (wt/wt) fat (lard) and 37% carbohydrate (primarily sucrose) [9]. B16 melanoma tumor cells (ATTC) were then injected into the subcutaneous space of both the axillary area and the inguinal area at a concentration of 5×10^5 cells per site. All mice were palpated daily to monitor tumor development. Primary tumors were measured in 2 dimensions using calipers and tumor volume calculated as length × width^2 × π/6. Mice were euthanized 14 days following tumor implantation, tumors were collected and tumor burden calculated as the per cent of tumor volume per body weight.

For evaluating metastatic response, XRCC1tp mice were crossed with PyMT transgenic mice on the FVB genetic background to generate F1 mice. The PyMT transgenic mouse is a widely used preclinical model to study metastatic breast cancer with a near 100 per cent metastasis to the lungs. Although the PyMT gene is not expressed in human breast cancer cells, its products bind to, and activate several signaling pathways such as Src, Ras and PI3 kinase, which are all implicated in human breast cancer. The PyMT model also demonstrates loss of estrogen and progesterone receptors, in addition to expressing ErbB2/Neu during the late carcinoma stage, both of which resemble human breast cancer with poor prognosis [10]. F1 mice were monitored for tumor onset and size and euthanized at 110 days and tissues collected into formalin and frozen for further evaluation. Tumor volumes were calculated as length × width^2 × π/6.

XRCC1 null heterozygous mice were obtained from Dr. Robert Tebbs, Lawrence Livermore National Laboratory, Livermore, CA, and backcrossed onto the C57BL/6 background for these studies.

All studies on mice complied with the Institutional Animal Care and Use Committee regulations approved by the University of Washington. Animals were kept in ventilated cages (4-5 per cage) in a specific pathogen free facility at the University of Washington. Mice were fed standard chow and provided reverse osmosis water.

All supplies entering the facility were autoclaved. Rooms were kept at a 12-hour light/dark cycle, maintained at 70-74 degrees F, 45-55% humidity with 28 changes per hour.

Caspase 3 immunohistochemistry

Caspase 3 is a marker for apoptotic activity. To identify cells expressing caspase 3, formalin-fixed mammary gland sections were immunostained using rabbit polyclonal to caspase 3 (Abcam, Cambridge, MA) as described [11]. Slides were deparaffinized for 30 minutes at 60°C. Endogeneous peroxidase activity was blocked using Leica Bond Peroxide block. Sections were incubated for 20 minutes using diluted normal blocking serum, followed by adding rabbit anti-caspase 3 or rabbit isotype to respective slides for 15 min. Specific reactivity was detected using Leica Bond Polymer DAB Refine for 8 minutes at room temperature and Leica Bond Mixed Refine for 10 minutes at room temperature. Tissues were counterstained for 10 seconds in hematoxylin followed by two rinses in H_2O and cleared with xylene. The number of caspase 3 labeled cells was determined by counting positive cells in a grid of eight squares encompassing the entire plane of view at 20X magnification per slide. The caspase 3 labeling index was calculated as the average per cent positive cells.

Exposure of cells to methyl methane sulfonate (MMS)

Primary lung fibroblast cells were treated with 0, 25, 30, 35, 40, 45, 50, 55, 60, 65 and 70 μg/ml of MMS (Sigma, St. Louis, MO), in growth media/10% FBS (5 wells/treatment). Five wells without cells and 0 μg/ml MMS were also used as an additional control. After being incubated with their respective treatments for 24 h at 37 degrees C in a humidified atmosphere with 5% CO_2, all wells were replaced with 100 μl of fresh media/10% FBS. Cells were allowed to recover for another 48 h at 37 degrees C in a humidified atmosphere with 5% CO_2. 10 μl of Cell Proliferation Reagent WST-1 (BD Biosciences, Mountain View, CA) was added to each well (1:10 final dilution) and cells were put back in the incubator for another 1.5 h. Plates were then shaken thoroughly on a shaker, and the absorbance of each of the wells was measured using a microplate reader at 450 nm. Wells without cells were used as a blank.

DNA repair assay

We measured kinetics of repair of alkylation damage to DNA in primary mouse fibroblast culture cells treated with MMS. Fibroblasts were derived from lung tissue (for XRCC1 L360R variant cells) or from ear tissue (for XRCC1 +/- heterozygotes). The assay was performed by *in vivo* labeling long stretches of genomic DNA with 50 uM IdU or CldU, then treating cells with the alkylating agent MMS (0.2 mg/ml for 10min) and taking a time course of recovery. High molecular weight genomic DNA was prepared via a standard agarose embedding procedure as described [12]. To generate breaks at sites of MMS lesions, cells in agarose plugs were lysed at 56 degrees C for 18 hrs. Subsequent treatments were done as described [13]. Briefly, genomic DNA was released from agarose, stretched on silanized glass cover slips, stained with anti IdU antibody (BD Biosciences) and anti CldU antibody (Abcam) and then with Alexa-conjugated secondary antibodies (Alexa 594 for CldU and Alexa 488 for IdU, respectively). Merged two-color images of tracks were generated using Axiovert fluorescent microscope (Carl Zeiss). Lengths of 150-800 each of IdU or CldU labeled tracks in DNA were measured off digital images using AxioVision software (Carl Zeiss). Significance of the differences was estimated in a KS test.

NAD/NADH assay

This assay uses the tetrazolium salt WST-1 and an electron coupling reagent to indirectly measure PARP activity (by measuring NADH availability and depletion) upon acute exposure to the DNA alkylating agent MMS, as described [14]. Briefly, mouse lung fibroblasts were cultured in DMEM with 10% fetal bovine serum and 1% Pen/Strep (Invitrogen). Cells were maintained in a humidified atmosphere at 37 degrees C in 5% CO_2. Mutant and wild type lung fibroblasts were plated at 4×10^3 cells per well in 100ul of medium, five wells per MMS concentration tested. Cells were then allowed to adhere overnight. The next day, medium was aspirated for the wells and medium containing the indicated concentration of MMS was added to the appropriate wells. Control wells (containing cells) and the blank control well (containing no cells) had medium with PBS added instead of MMS. Immediately after this, 10ul of WST-1 was added to each well. Readings were taken every 15

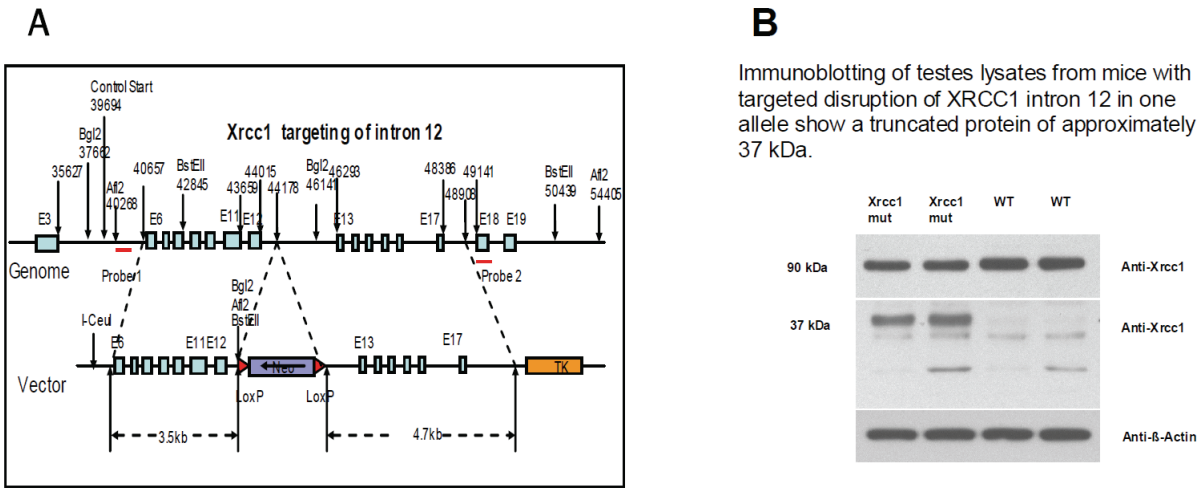

Figure 1. Generation of the XRCC1 mutant mice. (A) The gene targeting strategy consisted of a neomycin cassette targeting vector inserted into intron 12. (B) Western immunoblot shows a truncated protein of approximately 37 kDa.

minutes during the 1 hour and 30 minute period after addition of WST-1 using a Labsystems Multiskan microplate reader at a wavelength of 450nm. The OD value of the blank control was subtracted from all other OD values to eliminate background signal. The mean value of the OD readings from the control wells of each cell line was considered 100% of the available NADH. OD values of the treated cells were expressed as a percentage of their control.

Statistical analysis

Statistical analyses were performed using Student's t-test and two-tailed distribution unless otherwise specified. Statistical significance was defined when $p<0.05$. All results are presented as mean ± SD unless otherwise indicated. The percentage of tumor burden and tumor volume in each group was analyzed.

Results

XRCC1 intron 12 targeted mice express a truncated protein

Mutant mice were generated from C57BL/6 ES cells transfected with a neomycin cassette targeting vector (**Figure 1A**). The original intent was to generate mice expressing the L360R point mutation in the BRCT1 domain, so PCR primers were designed to detect this. Male chimeras were identified by coat color and genotyping, and then crossed with C57BL/6 wild type females. Heterozygous offspring were viable with no outwardly visible phenotype. However, when heterozygous mice were intercrossed with each other, no homozygous pups were detected by PCR genotyping in the original founder offspring or offspring from subsequent heterozygous breeding pairs (data not shown). The embryonic lethality suggested that the mouse line was a gene deletion mutation caused by insertion of the neomycin cassette in intron 12 rather than a point mutation. Western immunoblotting indicated the presence of a 37 kDa truncated protein (**Figure 1B**), which confirmed our suspicions. Since the presence of a truncated protein for the XRCC1 protein was a unique finding, it was of interest to pursue a phenotype for the mouse line, which we designated as XRCC1tp. All experiments described in this paper were done using heterozygous mice.

Cells from XRCC1tp mice maintain functional DNA repair but are hypersensitive to MMS

Since XRCC1 is part of the pathway involved in repairing damaged DNA, especially damaged bases and single strand breaks, it was of interest to determine if the repair process was compromised. We quantified repair of alkyl adducts based on breakage susceptibility of genomic DNA damaged by MMS (**Figure 2A**). Breakage susceptibility was assessed by measuring lengths of genomic DNA fragments stretched on siliconized glass [13, 15]. We show that primary lung fibroblasts from XRCC1tp mice do not de-

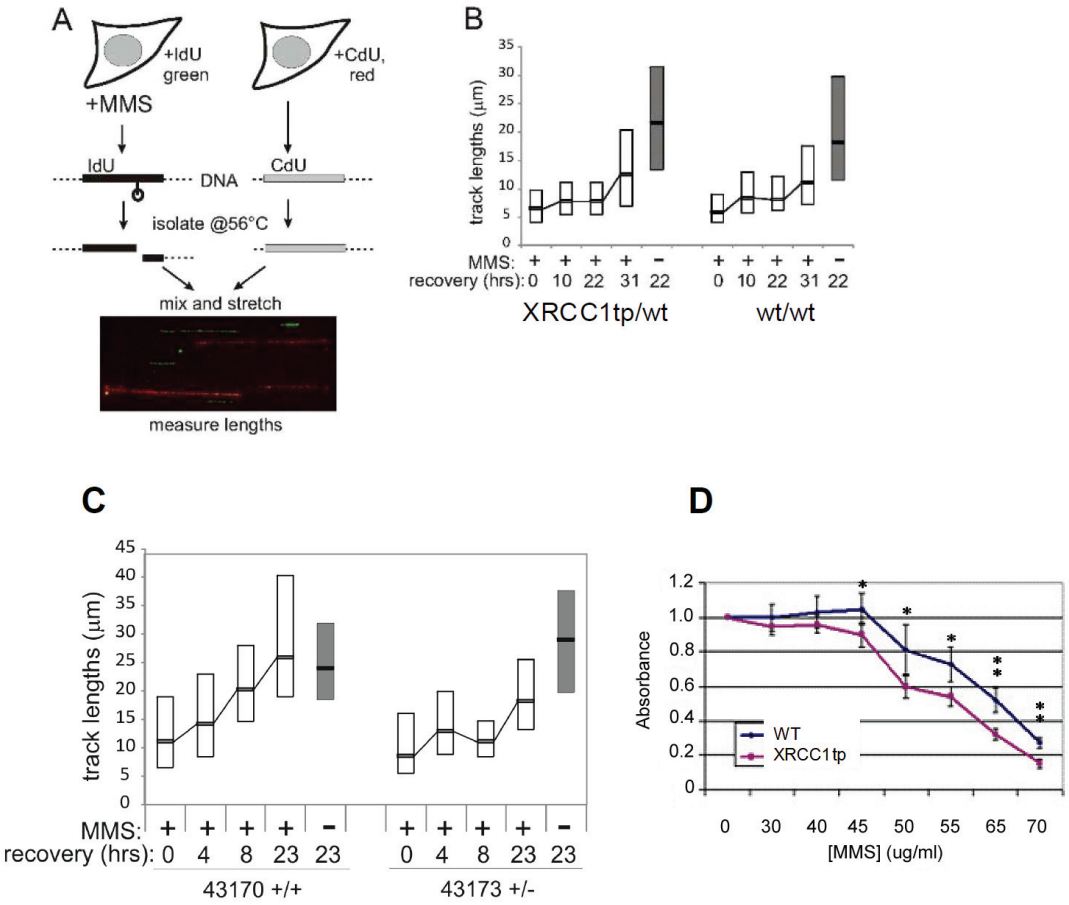

Figure 2. Primary mouse lung fibroblasts expressing XRCC1truncated protein are able to repair alkyl lesions. (A) A diagram of the experimental procedure shows that cells were labeled with IdU or CldU for 100 min, and then IdU-labeled cells were treated with 0.2 mg/ml MMS for 10 min. Time points were taken at 10, 22, and 31 hrs of recovery for IdU labeled cells and at a time point equivalent to 23 hrs of recovery for CldU-labeled controls. (B) Box plots of length distributions of labeled tracks in DNA from cells treated with MMS (white) or untreated controls (gray). Lower and upper box margins mark values corresponding to the first and third quartiles of distributions, respectively. Gray lines mark medians of distributions. Length distributions of tracks in the CldU-labeled DNA control in each series was measured repeatedly with each IdU-labeled sample shown, rendering similar profiles. Only one example of those profiles per genotype is shown in the Figure (gray bars). 150-800 labeled tracks were measured in each sample. (C) Primary mouse ear fibroblasts derived from an XRCC1 wild type mouse (43170+/+) and an XRCC1 null heterozygous mouse (43173+/-) show different rates of repair of alkyl lesions generated by MMS. Only one example of those profiles per genotype is shown (gray bars). (D) Primary lung fibroblasts from mice expressing XRCC1 truncated protein treated with MMS have reduced survival (absorbance) compared to primary lung fibroblasts from wild type littermates. *$p \leq 0.05$; **$p \leq 0.01$.

lay DNA repair compared to wild type controls (**Figure 2B**). As can be seen at 5, 10, 22, and 31 hours there is no significant difference in DNA repair in XRCC1tp fibroblast cells compared to WT cells exposed to MMS. This observation is in contrast to data from XRCC1 variant CHO cells that showed a delay in DNA repair using the comet assay [16], and might reflect different measurement endpoints. The stretched DNA display assay did detect a marked delay in repair of damaged DNA in XRCC1 null heterozygous cells (**Figure 2C**) indicating the ability of the assay to detect DNA repair deficiencies.

A hallmark phenotype of XRCC1 mutant CHO cells is hypersensitivity to MMS [16], so it was of interest to see if mouse cells expressing the XRCC1 truncated protein were sensitive to MMS, especially since they were able to functionally repair MMS-induced DNA damage. We

show that primary lung fibroblast cells carrying XRCC1tp are more sensitive than wild type littermate cells to MMS exposure (**Figure 2D**). These data suggest that expression of XRCC1tp disrupts the ability of XRCC1 to promote cell survival following MMS treatment similar to what has been reported for XRCC1 mutant CHO cell lines [16], but may not be associated with the DNA repair machinery. More likely, the mechanism relates to the function of XRCC1 in cell cycle control and cell death.

NADH is hyper-depleted in cells from mice expressing XRCC1tp

XRCC1 is recruited to SSB sites by PARP, where it has been reported to negatively regulate poly ADP-ribosylation [17], and thus prevent excessive PARP activity. It was therefore of interest to investigate the ability of cells expressing XRCC1tp to affect PARP function. We used an indirect assay based on NADH levels. PARP activity is NADH dependent so that when NADH levels are depleted, in this case by MMS-induced DNA damage, PARP is activated. As can be seen in **Figure 3**, NADH was depleted in a dose dependent manner after exposure of wild type lung fibroblasts to MMS. However, the depletion of NADH in cells with XRCC1tp was significantly enhanced. Because NADH levels returned to near normal in the presence of the PARP inhibitor 3AB, and there was no evidence of non-viable cells as determined by trypan blue staining, we conclude that the depletion is associated with PARP activity. These data are similar to observations made with XRCC1 mutant CHO cell lines [14], and suggest that the XRCC1 truncated protein is unable to maintain PARP in an inactive state.

Carcinogen-induced tumor growth is suppressed in XRCC1tp mice

Since XRCC1tp cells were shown to be sensitive to MMS, we tested the concept that XRCC1tp mice would be sensitive to another alkylating agent, azoxymethane (AOM), known to induce tumors in the colon of mice. XRCC1tp mice treated with AOM had a 54 percent incidence of colon tumors compared to a 46 percent incidence in wild type littermates, but the difference was not significant. Interestingly, the average colon tumor volume of 14.2 ± 3 cubic mm in XRCC1tp mice treated with AOM (representative tumor is shown in **Figure 4A**) was significantly less than the average colon tumor volume of 34±4 in wild type littermates treated with AOM (representative tumor shown in **Figure 4B**), $p \leq 0.03$. Histologically, the lesions in XRCC1tp mice were mainly adenomatous polyps and adenomas (**Figure 4C**) whereas the lesions in XRCC1 wild type littermates were mainly adenomas and adenocarcinomas *in situ* (**Figure 4D**), with an increase in mitotic figures. We did not see any evidence of invasion either locally or metastatically. These observations suggest that cell proliferation is being down regulated by expression of the XRCC1 truncated protein, and that the stromal microenvironment may be involved, since tumor incidence was not affected.

XRCC1tp has generalized anti-tumor activity

We used two well characterized mouse cancer models, implantable B16 melanoma and transgenic PyMT breast cancer, to see if the anti-tumor effect was a generalized phenomenon or if it was specific to alkylation induced carcino-

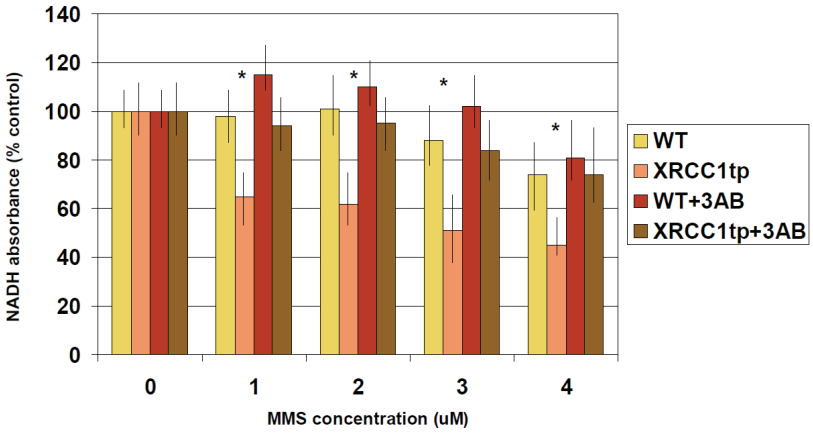

Figure 3. Depletion of NADH is enhanced in primary lung fibroblasts from mice expressing the XRCC1 truncated protein exposed to MMS for 30 minutes compared to primary lung fibroblasts from wild type (WT) littermates (*$P \leq 0.05$). The depletion is blocked by 3AB, a PARP inhibitor, showing that the decrease is associated with increased PARP activity.

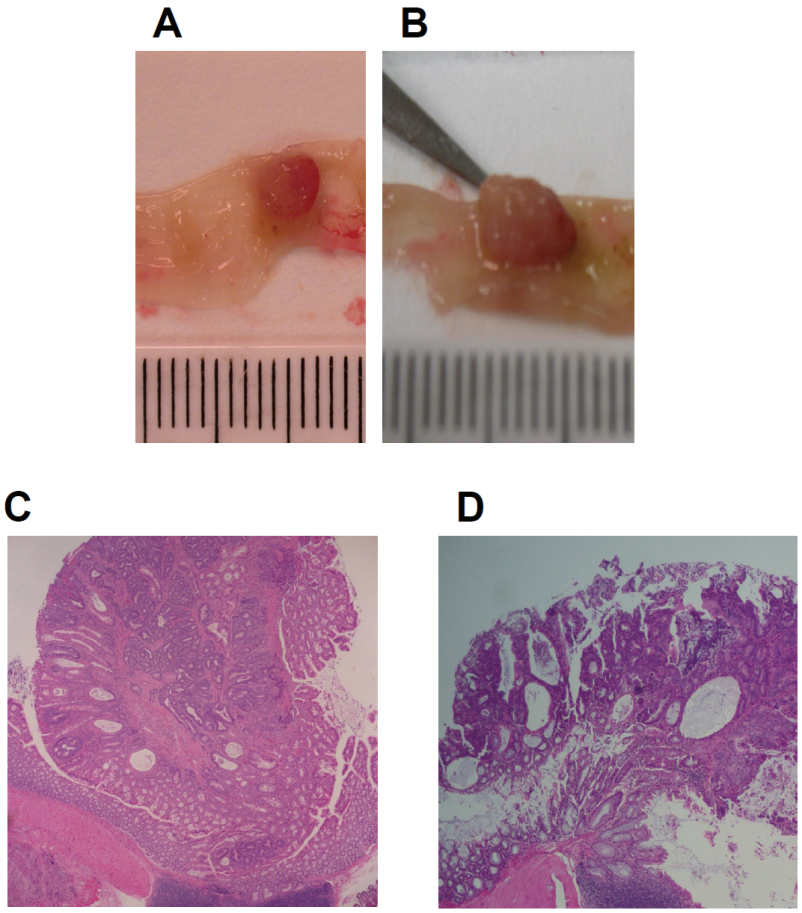

Figure 4. Colon tumor volumes in XRCC1tp mice given azoxymethane are significantly less than colon tumor volumes in wild type littermates given azoxymethane. The average colon tumor volume for eighteen XRCC1tp mice was 14.2±3 cubic mm as represented by (A). The average colon tumor volume for eighteen wild type mice was 34±4 cubic mm, represented by (B). The difference was statistically significantly at $p \leq 0.03$. Histologically, tumors from XRCC1tp mice were generally characterized as adenomatous polyps or adenomas (C), while tumors from XRCC1 wild type littermates were generally characterized as adenomas and adenocarcinomas in situ (D).

genesis. We implanted B16 melanoma cells subcutaneously into the axillary and inguinal spaces of seven XRCC1tp mice and six wild type littermates and showed a 72 per cent reduction in tumor burden in the XRCC1tp mice compared to wild type littermates, $p \leq 0.02$ (**Figure 5**). Since we had previously shown that tumorigenesis is enhanced in mice fed a high fat diet [18] we also implanted B16 melanoma cells into an additional cohort of mice fed a high fat diet for two months. Interestingly, the suppressive effect of XRCC1tp was attenuated in mice fed the high fat diet. These studies suggest that expression of XRCC1tp suppresses tumor growth by a mechanism possibly mediated by tumor stromal cells, and that this suppression is sensitive to dietary factors.

We then used the transgenic PyMT mouse model of metastatic breast cancer to see if XRCC1tp could affect metastasis. We have previously shown this model on the FVB x C57BL/6 F1 background to have an approximately eighty

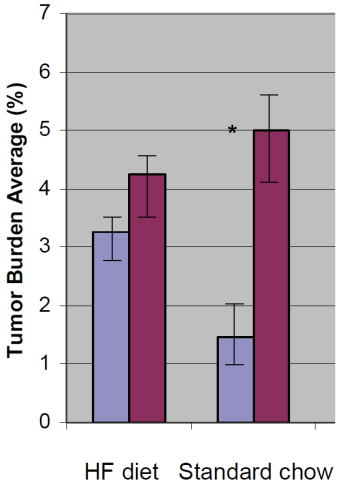

Figure 5. B16 melanoma tumor burden is significantly less in XRCC1tp mice (blue bars) fed standard rodent chow compared to WT littermates (red bars) fed the same diet (*$p \leq 0.02$, N = 10 per genotype). The tumor suppressive effect is abolished when these genotypes are fed a high fat (HF) diet (N = 10 per genotype).

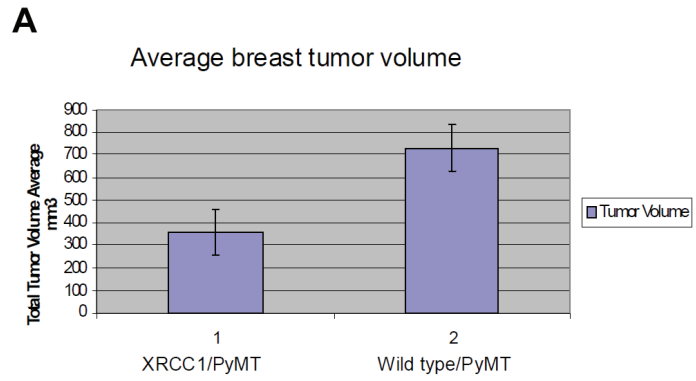

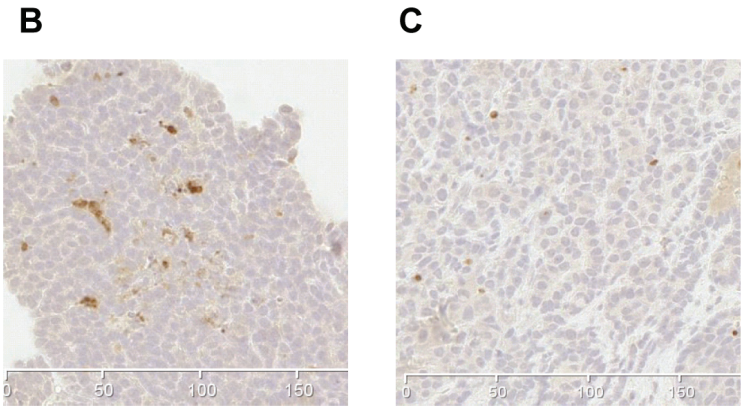

Figure 6. PyMT transgenic mice crossed with XRCC1tp mice have decreased breast tumor volume compared to PyMT transgenic mice crossed with wt mice, $p \leq 0.001$ (A). Primary tumor cells from PyMT x XRCC1tp F1 mice have increased labeling with caspase 3 (B), compared to primary tumor cells from PyMT x wt littermates (C), suggesting increased apoptopsis mediated by XRCC1tp.

per cent incidence of metastasis to the lungs [19]. PyMT mice were crossed with XRCC1tp mice and offspring identified as PyMT expressing XRCC1tp (N=19) or expressing XRCC1 wild type (N=20). The average time of onset of palpable tumors was 71 days with an incidence of 100% for mice in both cohorts. When mice were terminated at 110 days, average primary tumor volume was 359 cubic mm in PyMT mice expressing XRCC1tp compared to 730 cubic mm in PyMT mice expressing XRCC1wt ($p \leq 0.001$) (**Figure 6A**). A possible mechanism to help explain the decreased tumor volume may be increased cell death by apoptosis, since PyMT primary tumor cells expressing XRCC1tp had an increased caspase 3 labeling index of 19.6 per cent compared to 4.3 per cent for wild type tumor cells, $p \leq 0.01$ (**Figures 6B** and **6C**, respectively). When the lungs were examined histologically by micromorphometry for metastatic foci, PyMT mice expressing XRCC1tp had a 22 per cent incidence of metastasis while PyMT mice expressing XRCC1wt had an incidence of 79 per cent significant at $p \leq 0.01$, clearly indicating that XRCC1tp has an anti-metastatic effect, in addition to its suppressive affect on primary tumor cells.

Discussion

Complete XRCC1 gene deletion (null knock out) in mice results in embryonic lethality, demonstrating the protein is essential for development [20]. We have demonstrated that when the XRCC1 truncated protein (XRCC1tp) is expressed on both alleles, embryos also die before birth. We have not determined the exact time of death, but preliminary genotyping failed to detect any homozygous fetuses beyond day 10 similar to XRCC1 null mice, which show embryonic death at day 8. In contrast to the severe phenotype of homozygous mice, heterozygous XRCC1tp mice do not show any observable biological phenotype. These mice develop normally, and mature to adulthood without any problems. XRCC1tp mice have one wild type allele that maintains viability. We therefore were able to investigate functional effects and tumor response of these mice under a variety of conditions.

We first showed that primary lung fibroblast cultures expressing XRCC1 truncated protein were sensitive to the toxic effects of the akylating agent MMS. This observation directly implicates XRCC1 as a critical factor in promoting cell survival following MMS treatment. It is known that XRCC1 is required to allow unperturbed replication and progression through S phase after DNA damage so it is possible that disruption of cell cycle progression may allow cells to suffer the effects of direct alkylation toxicity and subsequent necrotic death. We

used a novel approach to measure repair of alkyl adducts in vivo by taking advantage of stretched DNA technology [13]. The assay provides a more sensitive readout of the molecular events in DNA repair compared to the Comet assay [5, 21] and has the advantage of quantitating repair efficiency. Expression of the XRCC1 truncated protein did not affect the ability of cells to repair MMS-induced DNA damage, suggesting that any phenotype observed in XRCC1tp mice would not be related to DNA repair function.

It was of interest to see if PARP activity was affected because the neomycin cassette had been inserted into intron 12 close to the coding region for the BRCT1 domain, which has been shown to be the area used by XRCC1 to interact with PARP [22]. We showed that cells expressing the XRCC1 truncated protein had an enhanced PARP-specific depletion of NADH suggesting increased PARP activity. It had previously been shown that reduced levels of XRCC1 are associated with an increased intracellular depletion of NADH, due to enhanced PARP activity [14, 15], and we now show the same results in XRCC1 truncated protein cells. This observation in fact supports a role of XRCC1 as a negative regulator of PARP activity as was suggested by Masson et al [17] who showed that overexpression of XRCC1 in HeLA cells resulted in impaired poly (ADP-ribose) synthesis in response to DNA damage. The biological consequences of alteration in PARP activity may be associated with as yet unknown mechanisms involved in the anti-tumor phenotype described in this paper.

AOM is metabolically activated in the liver by CYP 2E1, which converts it to methylazoxymethanol as the active compound for DNA adduct formation and tumor initiation. We expected that XRCC1 mutant mice would develop more progressive colon tumors in response to AOM, but the opposite occurred, with a significant decrease in colon tumor volume. It is possible that hepatic toxicity decreased the metabolic breakdown of AOM so that there was less active carcinogen available to act on the colonocytes. We suggest this is not the case for several reasons. First, there was no difference in incidence and numbers of tumors between the two genotypes, so if there was less active carcinogen, there would be an expected decrease in initiation. Second, we have shown that the XRCC1tp suppresses invasive tumors in non-carcinogenic mouse cancer model systems including B16 melanoma implanted tumors and metastatic breast cancer in PyMT transgenic mice. Although we do not know the mechanism for this suppression, the fact that B16 melanoma tumor growth was suppressed suggests stromal cell involvement. It is possible that the increased apoptosis we observed in primary breast tumors in PyMT transgenic mice expressing XRCC1tp is mediated by stromal cell signaling. Additional studies are needed to further investigate these initial and intriguing observations.

Acknowledgments

This work was funded in part by NIEHS grant R21ES016572-02 (Ladiges) and a pilot grant from the NIA-supported University of Washington Nathan Shock Center (Sidorova). Dr. Pettan-Brewer was supported by a Diversity Training Grant from NIA. The authors declare that there are no conflicts of interest.

Address correspondence to: Dr. Warren C. Ladiges, Department of Comparative Medicine, School of Medicine, University of Washington, Seattle, WA 98195, BOX 357190 Tel: (206) 685-3260; Fax: (206) 685-3006; E-mail: wladiges@u.washington.edu

References

[1] Thompson LH, West, MG. XRCC1 keeps DNA from getting stranded. Mutat 2000; 459: 1-18.

[2] El-Khamisy SF, Masutani M, Suzuki H, Caldecott, KW. A requirement for PARP-1 for the assembly or stability of XRCC1 nuclear foci at sites of oxidative DNA damage. Nucleic Acids Res 2003; 19: 5526-5533.

[3] Ladiges WC. Mouse models of XRCC1 DNA repair polymorphisms and cancer. Oncogene 2006; 25: 1612-1619.

[4] Intano GW, McMahan CA, McCarrey JR, Walter RB, McKenna AE, Matsumoto Y, MacInnes MA, Chen DJ, Walter CA. Base excision repair is limited by different proteins in male germ cell nuclear extracts prepared from young and old mice. Mol Cell Biol 2002; 22: 2410-2418.

[5] Horton JK, Watson M, STefanick DF, Shaughnessy DT, Taylor JA, Wilson SH. XRCC1 and DNA polymerase beta in cellular protection against cytotoxic DNA single-strand breaks. Cell Res 2008; 18: 48-63.

[6] MacAuley A, Ladiges WC. Approaches to determine clinical significance of genetic variants. Mutat Res 2005; 573: 205-220.

[7] Lamerdin JE, Montgomery MA, Stilwagen SA, Scheidecker LK, Tebbs RS, Brookman KW,

Thompson LW, Carrano AV. Genomic sequence comparison of the human and mouse XRCC1 DNA repair gene regions. Genomics 1995; 25: 547-554.
[8] Treuting P, Hopkins H, Ware C, Rabinovitch P, Ladiges W. Generation of genetically altered mouse models for aging studies. Experimental Mol Path 2002; 72: 49-55.
[9] Moore G, Knoblaugh S, Gollahon K, Rabinovitch P, Ladiges WC. Hyperinsulinemia and insulin resistance in Wrn null mice fed a diabetogenic diet. Mech Ageing Dev 2008; 9: 201-206.
[10] Lin EY, Jones JG, Li P, Zhu L, Whitney KD, Muller WJ, Pollard JW. Progression to malignancy in the Polyoma Middle T Oncoprotein mouse breast cancer model provides a reliable model for human diseases. Am J Pathol 2003; 163: 2113-2126.
[11] Ladiges WC, Knoblaugh SE, Morton JF, Korth MJ, Sopher BL, Baskin CR, MacAuley A, Goodman AG, LeBoeuf RC, Katze MG. Pancreatic β cell failure and diabetes in mice with a deletion mutation of the endoplasmic reticulum stress response gene P58IPK. Diabetes 2005; 54: 1074-1081.
[12] Herschleb J, Ananiev G, Schwartz DC. Pulsed-field gel electrophoresis. Nat Protoc 2007; 2: 677-684.
[13] Sidorova JM, Li N, Schwartz DC, Folch A, Monnat Jr RJ. Microfluidic-assisted analysis of replicating DNA molecules. Nat Protoc 2009; 4: 849 -861.
[14] Nakamura J, Asakura S, Hester SD, de Murcia G, Caldecott KW, Swenberg JA. Quantitation of intracellular NAD(P)H can monitor an imbalance of DNA single strand break repair in base excision repair deficient cells in real time. Nucleic Acids Res 2003; 31: e104.
[15] Lundin C, North M, Erixon K, Walters K, Jenssen D, Goldman ASH, Helleday T. Methyl methanesulfonate (MMS) produces heat-labile DNA damage but no detectable in vivo DNA double-strand breaks. Nucl Acids Res 2005; 33: 3799-3811.
[16] Taylor RM, Thistlethwaite A, Caldecott KW. Central role for the XRCC1 BRCT I domain in mammalian DNA single-strand break repair. Mol Cell Biol 2002; 20: 2556-2563.
[17] Masson M, Niedergang C, Schreiber V, Muller S, Menissier-de Murcia J, de Murcia G. XRCCC1 is specifically associated with poly(ADP-ribose) polymerase and negatively regulates its activity following DNA damage. Mol Cell Biol 1998; 18: 3563-3571.
[18] Pettan-Brewer C, Morton J, Mangalindan R, Ladiges W. Curcumin suppresses intestinal polyps in APC Min mice fed a high fat diet. Pathobiology Aging and Age-related Dis 2011; 1: 1-6.
[19] Goh J, Enns L, Fatemie S, Hopkins H, Morton J, Pettan-Brewer C, Ladiges W. Mitochondrial targeted catalase suppresses invasive breast cancer in mice. BMC Cancer 2011; 11: 191.
[20] Tebbs RS, Flannery ML, Meneses JJ, Hartmann A, Tucker JD, Thompson LH. Requirement for the Xrcc1 DNA base excision repair gene during early mouse development. Dev Biol 1999; 208: 513-529.
[21] Collins AR. The comet assay for DNA damage and repair: principles, applications, and limitations. Mol Biotechnol 2004; 26: 249-261.
[22] Caldecott KW. Cell signaling. The BRCT domain: signaling with friends? Science 2003; 302: 579 -580.